Cis-Trans isomerisation of azobenzenes studied by laser-coupled NMR spectroscopy and DFT calculations

Post-print of a peer-reviewed article published by the Royal Society of Chemistry.
Published article available at: http://dx.doi.org/10.1039/C0PP00056F

Cite as:
Wazzan, N. A., Richardson, P. R., & Jones, A. C. (2010). Cis-Trans isomerisation of azobenzenes studied by laser-coupled NMR spectroscopy and DFT calculations. *Photochemical & Photobiological Sciences*, 9(7), 968-974.

Manuscript received: 11/03/2010; Accepted: 26/04/2010; Article published: 24/05/2010

Cis-Trans Isomerisation of Azobenzenes Studied by Laser-Coupled NMR Spectroscopy and DFT Calculations**

Nuha A. Wazzan,[1] Patricia R. Richardson[1] and Anita C. Jones[1,*]

[1]EaStCHEM, School of Chemistry, Joseph Black Building, University of Edinburgh, West Mains Road, Edinburgh, EH9 3JJ, UK.

[*]Corresponding author; e-mail: a.c.jones@ed.ac.uk, tel: +44 1316506449. fax: +44 1316506453

[**]We gratefully acknowledge the support of the government of Saudi Arabia in the provision of a scholarship for NAW, the EaStCHEM computational facility and the Edinburgh School of Chemistry NMR facility.

Supporting information:
Electronic supplementary information (ESI) available: NMR spectra. See http://dx.doi.org/10.1039/C0PP00056F

Graphical abstract:

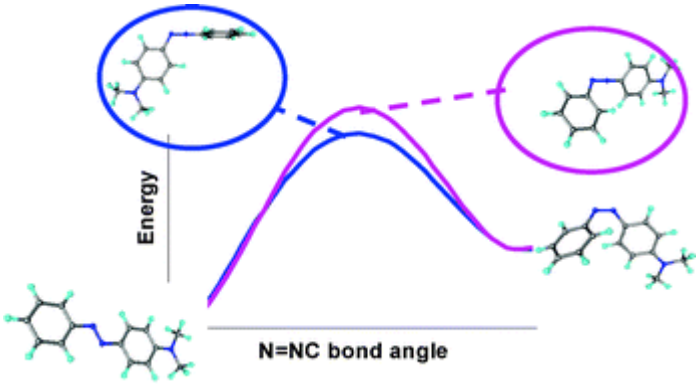

Abstract

In a combined experimental and computational study of a group of *para*-substituted azobenzenes, the effects of substituents and solvent on the kinetics of thermal *cis*-to-*trans* isomerisation have been examined and the success of DFT calculations in predicting kinetic parameters assessed. Mono-substituted species are predicted to isomerise by inversion in both non-polar and polar solvent, whereas for push-pull azobenzenes the mechanism is predicted to change from inversion to rotation on going from non-polar to polar solvent. Computed free energies of activation qualitatively reproduce experimental trends but do not quantitatively predict the kinetics of *cis*-*trans* isomerisation. The polarisable continuum model of solvation fails to predict the experimentally observed influence of solvent on the entropy of activation.

Introduction

In 1937, Hartley[1] published the first piece of work characterising the species resulting from the exposure of a solution of azobenzene to light, thus identifying for the first time the photochemical isomerisation of azobenzene. Since then the photoisomerisation of azobenzene has become a paradigm of unimolecular photochemistry and investigation of the mechanism of the excited state *trans*-*cis* isomerisation has been a popular subject for ultra-fast spectroscopy. In this paper we are concerned with the thermally induced conversion of the *cis* photoisomer back to the thermodynamically stable *trans* form. The mechanism of the ground state process has received less attention than the photoisomerisation, but is equally controversial. On the basis of experimental studies examining the effects of factors such as substituents, solvent polarity, pH and pressure, on the reaction kinetics, conflicting claims have been made for the two alternative mechanisms, inversion about one of the azo nitrogens or rotation about the azo double bond.[2-13] It is envisaged that inversion proceed *via* a linear transition state (TS) in the which the N-N double bond remains intact, whereas rotation proceeds *via* a twisted transition state in which the N-N π-bond is broken. Frequently the interpretation of experimental data has been based on the argument (from resonance structures) that the rotational TS would be dipolar but the inversion TS would not.

Azobenzenes have long been used as dyes and colourants, but more recent applications have sought to exploit the ability to photoswitch the geometric, electronic and optical properties of the molecule. Such applications include memories and switches in new electronic and photonic systems,[14,15] photoswitches to affect various physical properties of materials,[16,17] and components in molecular machines.[18] The longevity of the photogenerated *cis* isomer is of relevance in both traditional and new applications. In dyeing and printing, the formation of a *cis* product that is long-lived is disadvantageous since it results in a pronounced photochromic effect and the constancy of the colour is weakened. On the other hand, the synthesis of azo dyes with long-lived *cis* isomers is required for modern applications in which conversion to the *trans* form should be entirely under photochemical control.

The ability to computationally predict the kinetics of thermal isomerisation from the molecular structure would be highly advantageous for the customised design of molecules for specific applications. Recently, Dokic *et al*[19] have reported a density functional theory (DFT) study of the *cis*-to-*trans* isomerisation of a wide range of azobenzene derivatives, as a step towards understanding the effect of surface-binding on the thermal isomerisation in molecular switching applications. However, this study included only a very limited set of experimental kinetic data on some tetra-*tert*-butyl-azobenzene derivatives. Thus the majority of the predicted rate constants and activation parameters reported remain untested experimentally. We now report a combined experimental and computational study of a group of *para*-substituted azobenzenes in which we examine the effect of substituents and solvent on isomerisation kinetics and assess the success of DFT calculations in predicting these effects. Experimental results are reported for 4-aminoazobenzene (AAB), 4-nitroazobenzene (NAB), disperse orange 3 (DO3), 4-dimethylamino-4'-nitroazobenzene (DMNAB) and disperse red 1 (DR1). One of the push-pull azobenzenes, DMNAB, was omitted from the computational study, but the parent molecule, azobenzene (AB), was included. The structures of the molecules are shown in Scheme 1. Experimental studies were carried out using laser-coupled NMR spectroscopy, in which the sample is irradiated *in situ* within the NMR probe and the intensity of the NMR signals due to the two isomers are monitored during the isomerisation process. DFT calculations were carried out using the B3LYP functional and the 6-31G(d,p) basis set, a higher basis set than the 6-31G* used by Dokic *et al*,[19] and the polarisable continuum model of solvation.

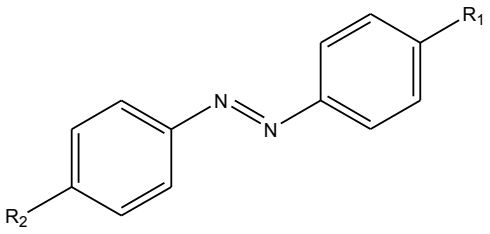

	R_1	R_2
AB	H	H
AAB	H	NH_2
NAB	H	NO_2
DO3	NO_2	NH_2
DMNAB	NO_2	$N(CH_3)_2$
DR1	NO_2	$N(CH_2CH_3)(CH_2CH_2OH)$

Scheme 1. Structures of the molecules studied: azobenzene (AB), 4-aminoazobenzene (AAB), 4-nitroazobenzene (NAB), disperse orange 3 (DO3), 4-dimethylamino-4'-nitroazobenzene (DMNAB) and disperse red 1 (DR1).

Experimental

Materials

The azobenzenes were obtained from Aldrich and used as received. No impurities were detected in the NMR spectra. Deuterated solvents, d_6-benzene and d_6-dimethylsulfoxide, were also obtained from Aldrich and used as received. Hereafter the solvents will be referred to as benzene and DMSO.

Measurement of rate constants and activation parameters

The kinetics of the thermal *cis*-*trans* isomerisation were investigated using NMR spectroscopy with *in situ* laser irradiation. The experimental system and general experimental procedure have been described previously.[20,21] The photostationary state was prepared by laser irradiation of the sample in the NMR probe until the intensity of signals due to the two isomers became constant. As reported previously[20-22] the signals of the two isomers can be readily distinguished. The *cis* isomer protons are consistently more shielded than their *trans* isomer counterparts and protons *ortho* to the azo linkage show particularly large differences in their chemical shifts in the two isomeric forms. As an example, the NMR spectra of the *trans* isomer and photostationary state of AAB and their assignments are given the Supporting Information.

A pseudo two-dimensional pulse programme was used to acquire the kinetic data. The F2 domain of the NMR spectrum was acquired as for a normal 1D spectrum using a presaturation pulse. The F1 domain was simply the time interval between successive 1D experiments. Changes in peak intensity as a function of time can thus be followed and the data extracted and fitted. Although this method is used primarily for t_1/t_2 relaxation experiments in NMR, this pulse programme is highly suitable for the kinetic experiments. Following attainment of the photostationary state, the conditions were optimised and a high quality spectrum of the PSS recorded, prior to monitoring thermal decay of the *cis* isomer. The first row of the 2D spectrum was recorded under irradiation, at t_0, after which irradiation was terminated allowing the *cis* isomer to decay in darkness. Periodic monitoring of the decay was conducted until no further changes were observed, ensuring the full thermal decay process was recorded.

The data were Fourier transformed in the F2 dimension only, F1 being the time dimension. The time interval is taken as the time that elapsed during the acquisition of each row. After the transformation of F2, the same phasing and baseline correction parameters were applied to each row of the data set. A 1D spectrum was extracted from the pseudo 2D file. *Trans* and *cis* signals were selected and the limits of integration for each peak defined. With these parameters defined, Xwinnmr software was used to extract the integral for the same peak in all rows of the 2D spectrum, giving an output that was suitable for fitting by the appropriate mathematical function.

The thermal relaxation of the *cis* isomer to the thermodynamically more stable *trans* form is described by first order kinetics. The time-dependence of the concentration of *cis* and *trans* isomers are given by

$$[cis]_t = [cis]_{PSS} \exp^{-kt} \qquad \textbf{Equation 1}$$

$$[trans]_t = [trans]_{PSS} + [cis]_{PSS}\left(1 - \exp^{-kt}\right) \qquad \textbf{Equation 2}$$

where $[cis]_t$ is the concentration of the *cis* isomer at time t, $[cis]_{PSS}$ is the concentration of the *cis* isomer at the photostationary state (PSS), $[trans]_t$ is the concentration of the *trans* isomer at time t, $[trans]_{PSS}$ is the concentration of the *trans* isomer at the PSS and k is the rate constant for thermal isomerisation.

Two data sets were extracted from the pseudo 2D data, one for the *trans* isomer integrals and one for the *cis* isomer integrals. These data were imported in Microsoft Excel and an iterative non-linear least square procedure was used to fit the data using the 'Solver' function. Data were fitted to the integrated first order rate laws given in Equations 1 and 2. Two estimates of the rate constant were thus obtained, one from the *cis* signal decay (Equation 1) and one from *trans* signal rise (Equation 2) during the thermal isomerisation. The rate constant reported is the averages of the values obtained from the pair of *trans* and *cis* data sets.

Activation parameters were determined by measuring the temperature dependence of the rate constant and fitting the data with the Arrhenius equation (Equation 3) or the Eyring equation (Equation 4) to obtain the activation energy, E_a, the enthalpy of activation, $\Delta H^{\ddagger}$, the entropy of activation, $\Delta S^{\ddagger}$ and the Gibbs free energy of activation, $\Delta G^{\ddagger}$. Measurements were taken typically in the temperature range 288 K to 328 K.

$$\ln k = \ln A - \frac{E_a}{RT} \qquad \textbf{Equation 3}$$

where k is the thermal rate constant, R is the universal gas constant, T is the temperature in Kelvin, A is the steric factor and E_a is the activation energy.

$$\ln \frac{k}{T} = \frac{-\Delta H^{\ddagger}}{RT} + \ln \frac{k_B}{h} + \frac{\Delta S^{\ddagger}}{R} \qquad \textbf{Equation 4}$$

where $\Delta H^{\ddagger}$ is the enthalpy of activation, $\Delta S^{\ddagger}$ the entropy of activation, k_B is the Boltzmann constant, h is Planck's constant.

The Gibbs free energy of activation, $\Delta G^{\ddagger}$, is given by

$$\Delta G^{\ddagger} = \Delta H^{\ddagger} - T\Delta S^{\ddagger} \qquad \textbf{Equation 5}$$

DFT Calculations

Calculations were performed using an AMD opteron-based cluster, running the *Gaussian* 03 package[23] under Linux. Geometry optimisations were conducted by density functional theory (DFT) using Beck's three parameter exchange functional[24], the Lee-Yang-Parr correlation functional[25] (B3LYP) and the 6-31G(d,p) basis set. In geometry optimisations every bond length, bond angle and dihedral angle was allowed to relax, free of constraints.

Potential energy curves (PEC) were constructed starting from either the *trans* or *cis* optimized geometry by constraining either the C-N=N-C dihedral angle or one of the C-N=N bond angles while optimizing all the other structural parameters. The constrained angle was incremented in 10-degree steps, between the *cis* and *trans* minima, and the energy of the optimised structure obtained at each point. The activation energy, E_a, quoted is the difference between the zero point energy of the *cis* isomer and that of the transition state (TS).

The nature of the stationary points (*cis* isomer, *trans* isomer and transition state) were confirmed by vibrational frequency analysis, to verify that only real frequency values were obtained for the two isomers and a single imaginary frequency was shown by the transition state. The thermochemical parameters, G, H and S for the cis isomer and the TS were obtained from the frequency calculations and used to calculate the activation parameters, $\Delta H^{\ddagger}$, the entropy of activation, $\Delta S^{\ddagger}$ and the Gibbs free energy of activation, $\Delta G^{\ddagger}$.

In addition to calculations on gas-phase species, calculations in two solvents, benzene and DMSO, were performed employing the self consistent reaction field (SCRF) method based on the polarisable continuum model (PCM).[26,27] The optimised structures of the *cis* and *trans* forms and transition state obtained from the PEC in the gas phase were re-optimised in the desired solvent. Vibrational frequencies were computed for the optimised solution-phase geometries, to confirm the nature of the stationary points and to obtain the thermochemical parameters.

Results and Discussion

Experimental Results

The rate constant and activation parameters for the thermal isomerisation of each molecule are given in Table 1. For AAB and NAB, measurements were made in both benzene and DMSO. However, for DO3, DMNAB and DR1 the rate of reaction in DMSO was too fast to be measured and we can only estimate lower limits for the rate constants. The rate constants for DO3 and DR1 in benzene are in good agreement with those reported in the literature for these molecules in similar solvents.[8,28] The activation parameters reported here are broadly consistent with values in the literature for various azobenzenes in various solvents,[8,4,6,29] but we are not aware of previous studies that are specifically comparable.

Table 1. The experimentally measured rate constants and activation parameters of the thermal isomerisation in benzene (normal font) and in DMSO (bold font). The values of k and $\Delta G^{\ddagger}$ were obtained at 298 K.

Molecule	k / 10^{-5} s^{-1}	E_a / kJ mol^{-1}	$\Delta H^{\ddagger}$ / kJ mol^{-1}	$\Delta S^{\ddagger}$ / J mol^{-1} k^{-1}	$\Delta G^{\ddagger}$ / kJ mol^{-1}
AAB	5.1	74.0	71.4	-88.1	97.7
	9.8	**114.8**	**112.28**	**54.4**	**96.1**
NAB	10.2	37.2	34.6	-205.5	95.9
	960	**91.7**	**89.2**	**17.7**	**84.0**
DO3	320	71.8	69.3	-60.7	87.4
	>5x10^3	-	-	-	-
DMNAB	1150	64.6	62.1	-73.5	84.0
	>10^4	-	-	-	-
DR1	2760	40.5	38.0	-147.3	81.9
	>5x10^4	-	-	-	-

For the parent molecule, azobenzene, in hexane at 293 K, the rate constant has been reported to be 3.0 x 10^{-6} s^{-1} and the values of $\Delta H^{\ddagger}$, $\Delta S^{\ddagger}$ and $\Delta G^{\ddagger}$ to be 88.7 kJ mol^{-1}, -50.2 J mol^{-1} k^{-1} and 103.7 kJ mol^{-1}, respectively.[4] It is evident that *para*-substitution, with an electron donor or acceptor, accelerates the rate of isomerisation, with a corresponding decrease in the free energy of activation. For the *para*-donor/*para*-acceptor substituted (push-pull) azobenzenes, DO3, DMNAB and DR1, the rate constant is increased by orders of magnitude relative to the mono-substituted and parent molecules.

In all cases rate of isomerisation is faster in DMSO than benzene; this is particularly marked for NAB and the push-pull azobenzenes. However, this does not arise from a decrease in the activation energy (enthalpy) in the polar solvent. Examination of the activation parameters for AAB and NAB shows that the increase in rate constant in going from benzene to DMSO is accompanied by an *increase* in the activation energy or enthalpy of isomerisation. The smaller rate constant (higher free energy of activation) in benzene correlates with a relatively large negative entropy of activation in this solvent, which is evident for all of the molecules, whereas the entropy of activation in DMSO is positive and relatively small. This effect of the solvent on the activation parameters is characteristic of a reaction in which there is an increase in dipole moment in the transition state[12,30,31] and can be explained qualitatively by considering the cybotactic region, the part of a solution in the vicinity of a solute molecule in which the ordering of the solvent molecules is modified by the presence of the solute molecule. For the non-polar, polarisable benzene molecules in the cybotactic region, an increase in the dipole moment of the azobenzene molecule (and hence in the dipole moments induced in the benzene molecules) on going from the *cis* isomer to the transition state will lead to a more ordered structure of the solvent molecules with a corresponding decrease in entropy. This is typically compensated by a decrease in enthalpy. For the polar DMSO, the degree of order in the solvent structure, and hence the entropy, will be relatively little influenced by changes in the dipole moment of the solute molecule. Thus the observation of

negative activation entropy and lower activation enthalpy in benzene indicates that the transition state is more polar than the *cis* isomer. This is borne out by the DFT calculations, as discussed below.

DFT Calculations

The nature of the transition state

Figure 1 shows the potential energy curve (PEC) calculated for the isomerisation of AAB in the gas phase by constraining the C-N=N-C dihedral angle to adopt fixed angles, from 0° to 180° degrees in 10° increments, and allowing all other geometrical parameters to optimise without constraint at each point. This reaction coordinate corresponds to torsion about the

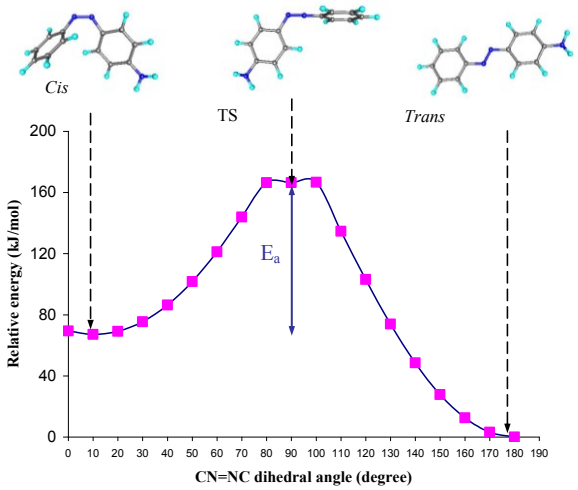

Figure 1. The computed potential energy curve for thermal isomerisation of AAB along a reaction coordinate corresponding to the C-N=N-C dihedral angle. The computed geometries of the *cis* and *trans* isomers and the transition state are also shown.

N=N bond and would be anticipated to lead to a rotation transition state. However, it can be seen that there is a dip in energy at the top of the potential energy curve and the transition state (TS) obtained has a linear N=N-C structure, i.e. it is an inversion TS. Similar behaviour has been reported previously for DFT calculations on DMNAB[28]. Once the dihedral angle exceeds 80°, the structure spontaneously optimises to the inversion TS by increasing the C-N=N bond angle to 180°. In this linear geometry, the C-N=N-C dihedral angle is not defined. We find that the same linear inversion TS is obtained by constraining isomerisation to occur along the inversion coordinate (constraining the C-N=N angle). By forcing isomerisation to proceed along the rotation

coordinate, by fixing the C-N=N angles at those of the ground state minimum energy structure, we access a rotation TS for AAB that is 38.5 kJ mol^{-1} higher in energy than the inversion TS. These findings are consistent with the recent DFT study (at the 6-31G(d) level) of Dokic *et al*[19] who carried out 2-dimensional scans of the isomerisation potential energy surface for a number of azobenzenes, varying both the dihedral and inversion angles. This demonstrated that along the lowest energy path to the linear transition state both of these angles change simultaneously. It was also found that the 2-dimensional potential energy surface supports several inversion pathways which go through maxima of similar height and isomerising along a pure inversion path has little effect on the activation energy.

The PEC of AAB shown in Figure 1 is typical of those found in the gas phase for all of the azobenzenes studied. In all cases an inversion TS state was found. For the asymmetric molecules (i.e. all except the parent azobenzene) there are two alternative inversion transition states. For NAB and the push-pull azobenzenes we find inversion about the azo nitrogen adjacent to the acceptor-substituted phenyl ring, while AAB inverts about the nitrogen adjacent to the unsubstituted ring. This is in complete agreement with the findings of Dokic *et al*[19] whose study included AB, AAB, NAB and DO3 in the gas phase. The structures of the transition states are shown in Figure 2 and the geometrical parameters of the azo linkage of the AAB TS are compared with those of the *cis* isomer in Table 2. The azo bond is shortened in the TS, as is the C-N bond that becomes linear with the N=N bond in the TS.

Table 2. Geometrical parameters of the azo linkage for the *cis* isomer and the transition state of AAB in the gas phase.

	Cis	TS
Bond length / Å		
N=N	1.254	1.230
(Ph)C−N(azo)	1.434	1.332
(NH_2Ph)C−N(azo)	1.427	1.435
Bond angle / ^{0}		
(Ph)C−N=N	124.3	180.0
(NH_2Ph)C−N=N	125.0	117.6
C−N=N−C (dihedral)	10.4	90.0

Figure 3 shows the PECs, along the dihedral rotation path, computed for AAB in benzene and DMSO (using the polarisable continuum model) in comparison with the gas-phase PEC. The predicted PECs in the solvated state are of the same form as in the gas phase and in solvated structures of the *cis* and *trans* isomers and the TS, the respective C-N=N-C dihedral angles do not differ significantly from the gas-phase structures. It was,

therefore, considered unnecessary to compute the entire PECs of all of the azobenzenes in the solvated states. Instead, the solvated structures of the two isomers and the TS were obtained by taking the optimised gas phase structure as the starting geometry, fixing the dihedral angle and reoptimising all other parameters, without constraint, in the presence of solvent.

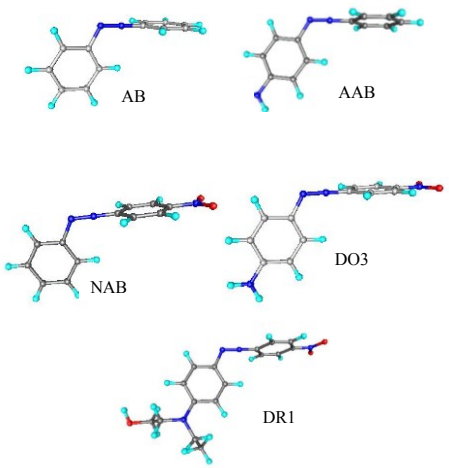

Figure 2. The calculated structures of the transition states of the azobenzenes in the gas phase.

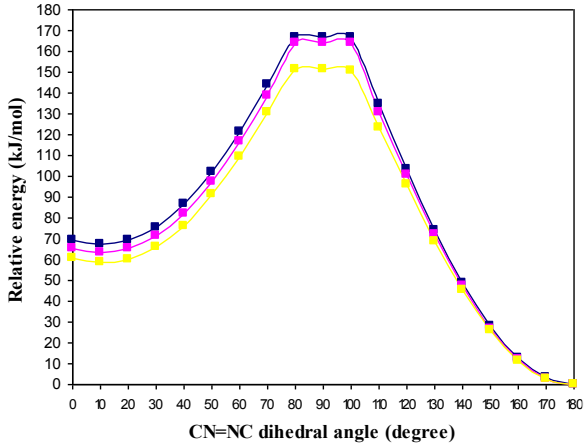

Figure 3. Comparison of the computed potential energy curves for thermal isomerisation of AAB along the C-N=N-C dihedral coordinate in the gas phase (blue), benzene (red) and DMSO (yellow).

In all cases, except DO3 and DR1 in DMSO, the solvated molecules were found to isomerise through the inversion TS. For AAB and NAB, in both solvents, the inversion TS was lower in energy than the rotation TS by 30 kJ mol^{-1} and 40 kJ mol^{-1}, respectively. For DO3 and DR1 in benzene the difference in energy was reduced to 18 kJ mol^{-1} and 13 kJ mol^{-1}, respectively. For both DO3 and DR1 in DMSO, the TS was found to be of the rotation type, as shown in Figure 4. Previously, Dokic *et al* also found an inversion TS for DO3 in

benzene, but a rotation TS in polar solvents including DMSO. Our identification of rotation transition states for both DR1 and DO3 in DMSO, suggests that the change in mechanism from inversion to rotation with increasing solvent polarity is a general feature of push-pull azobenzenes.

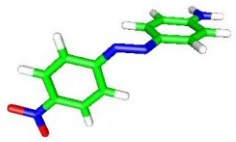

Figure 4. Structure of the rotation TS predicted for DO3 in DMSO.

As shown in Table 3, there is predicted to be a substantial increase in dipole moment between the *cis* isomer and the TS for all of the substituted azobenzenes. This is consistent with the conclusion drawn from the experimental data, based on the effect of solvent on the activation parameters. Moreover, it counters the notion that experimental evidence for a polar TS must imply the rotation mechanism. The particularly small activation energies and large negative activation entropies measured for NAB and DR1 in benzene (Table 1) correlate with the large relative increase in dipole moment, around a factor of 2, predicted for these systems. The polarity of the TS increases, in all cases, on going from benzene to DMSO, but this is particularly marked for DO3, where the nature of the TS changes from inversion in benzene to rotation in DMSO.

Table 3. Dipole moments for the optimised geometries of the *cis* isomers and the transition states in the gas phase (italic), benzene (normal font), and DMSO (bold).

Molecule	μ_{cis} / D	μ_{TS} / D
AB	*3.4*	*2.5*
	4.3	2.9
	5.2	**3.7**
AAB	*6.4*	*6.2*
	6.4	7.5
	8.3	**9.5**
NAB	*5.1*	*10.8*
	5.9	13.1
	6.6	**16.5**
DO3	*7.5*	*14.9*
	10.8	18.4
	11.1	**27.2**
DR1	*6.9*	*13.1*
	8.2	16.0

Activation parameters

The calculated activation parameters are given in Table 4. Consider first the predicted free energies of activation. The values of $\Delta G^{\ddagger}$ qualitatively reflect the decreasing trend seen in the experimental values (Table 1) on going down the table from AAB through NAB to the push-pull molecules. (The predicted value of $\Delta G^{\ddagger}$ for the parent molecule in the gas phase is 138.5 kJ mol^{-1} compared with a literature value[4] of 103.7 kJ mol^{-1}in cyclohexane.) The calculations also correctly predict similar values of $\Delta G^{\ddagger}$ in benzene and DMSO for AAB, but a significant decrease in DMSO for NAB. The predicted large decrease in $\Delta G^{\ddagger}$ on going from benzene to DMSO for the push-pull azobenzenes is consistent with the large acceleration in rate seen experimentally and correlates with the predicted change from inversion to rotation TS. However, although the trends are successfully reproduced, the magnitude of $\Delta G^{\ddagger}$ is significantly underestimated in all cases except AAB. The discrepancy ranges from about 10% to about 30% and leads to an overestimate of the rate constant by as much as four orders of magnitude.

Turning now to the enthalpy and entropy of activation. It is evident that the effect of the solvent on these parameters, which is so marked in the experimental results, is not manifested in the computational results. In almost all cases, in the gas phase and both solvents, small positive values of $\Delta S^{\ddagger}$ are predicted, so that $\Delta H^{\ddagger}$ and E_a approximate to $\Delta G^{\ddagger}$. Only in the case of DR1 in benzene is a significantly negative value of $\Delta S^{\ddagger}$ predicted, but this is much less than that observed experimentally. Given that the negative entropy of activation in benzene is attributed to the ordering of solvent molecules around the TS, it is perhaps not surprising that this behaviour is not reproduced by a computational model in which the solvent is treated as a continuum and which does not take account of solute-solvent interaction at the molecular level.

Table 4. The activation parameters predicted by DFT calculations for the azobenzenes in the gas phase (italic), benzene (normal font) and DMSO (bold). The value of $\Delta G^{\ddagger}$ was calculated at 298 K.

Molecule	E_a / kJ mol^{-1}	$\Delta H^{\ddagger}$ / kJ mol^{-1}	$\Delta S^{\ddagger}$ /J mol^{-1} K^{-1}	$\Delta G^{\ddagger}$ / kJ mol^{-1}
AAB	*94.1*	*94.3*	*7.2*	*92.1*
	95.4	95.7	7.9	93.3
	97.7	**98.1**	**10.8**	**94.9**
NAB	*76.6*	*76.1*	*0.22*	*76.3*
	73.2	72.9	-0.69	73.1
	68.6	**68.2**	**-3.2**	**69.1**
DO3	*69.5*	*69.5*	*1.6*	*69.0*
	64.4	64.6	9.1	61.8
	50.6	**49.4**	**-12.9**	**53.2**
DR1	*69.1*	*69.1*	*7.2*	*66.9*
	66.2	63. 7	-29.3	72.4
	53.7	**52.7**	**-9.9**	**55.6**

Conclusion

The rate of thermal isomerisation of azobenzene is accelerated by the introduction of an electron donating or electron accepting substituent in the *para*-position. For push-pull azobenzenes the rate is greatly increased relative to the parent and mono-substituted molecules. The rate of isomerisation of the push-pull azobenzenes in DMSO is greater by at least an order of magnitude than the rate in benzene. The marked effect of solvent properties on the activation parameters, $\Delta H^{\ddagger}$ and $\Delta S^{\ddagger}$, specifically the large negative activation entropy and reduced activation enthalpy in benzene, is clear evidence of a sizeable increase in dipole moment in the TS.

DFT calculations at the B3LYP/6-31G(d,p) level of theory, with solvent modelled as a polarisable continuum, predict that isomerisation proceeds by via a linear transition, i.e. by an inversion mechanism, for all cases except the push-pull azobenzenes in DMSO, which follow a rotation mechanism. These conclusions, are consistent with previous calculations performed at a lower level of theory (B3LYP/6-31G*), also using the PCM to treat solvation.[19] The predicted linear TS structures all possess substantially greater dipole moments than the corresponding *cis* isomer, in agreement with the experimental findings. Thus, experimental evidence for a dipolar TS should not be assumed to imply that isomerisation occurs by rotation.

Computed activation free energies qualitatively reproduce the trends seen experimentally on varying the substituents and solvent. However, at a quantitative level the calculations are less successful, tending to significantly underestimate the value of $\Delta G^{\ddagger}$, to the extent that, in some cases, the rate constant would be overestimated by as much a four orders of magnitude. The PCM treatment of solvation fails to reproduce the effect of solvent molecular order in the cybotactic region on $\Delta H^{\ddagger}$ and $\Delta S^{\ddagger}$. It remains to be seen if this effect can be successfully predicted by more sophisticated computational models of solvation in which interaction between solute and solvent molecules are treated explicitly.

We conclude that DFT calculations, at a moderate level of theory, provide valuable insight into the mechanism of thermal isomerisation, the structure of the TS and its polarity, assisting in the rationalisation of experimental kinetic data. Computed activation parameters may aid molecular design by qualitatively predicting the influence of substituents and environment on the lifetime of the *cis* isomer, but do not quantitatively predict the kinetics of *cis*-*trans* isomerisation.

References

[1] G.S. Hartley, *Nature (London, United Kingdom)* 1937, **140**, 281.

[2] S.F. Dietrich, *Justus Liebigs Annalen der Chemie* 1958, **615**, 114-123.

[3] E.R. Talaty, J.C. Fargo, *Chem.Commun.* 1967, **933**, 65-66.

[4] T. Asano, T. Okada, S. Shinkai, K. Shigematsu, Y. Kusano, O. Manabe, O. *J. Am. Chem. Soc.* 1981, **103**, 5161.

[5] D. Gegiou, A. Muszkat, J. Fischer, *J. Am. Chem. Soc.* 1968, **90**, 3907.

[6] N. Nishimura, T. Sueyoshi, H. Yamanaka, E. Imai, S. Yamamoto, S. Hasegawa, *Bull. Chem. Soc. Jpn* 1976, **49**, 1381-1387.

[7] N. Nishimura, S. Kosako, Y. Sueishi, *Bull. Chem. Soc. Jpn* 1984, **57**, 1617-1625.

[8] P.D. Wildes, J.G. Pacifici, G. Irick, D.G. Whitten, *J. Am. Chem. Soc.* 1971, **93**, 2004-2008.

[9] T. Sueyoshi, N. Nishimura, S. Yamamoto, S. Hasegawa, *Chem. Lett.* 1974, 1131-1134.

[10] N. Nishimura, S. Tanaka, Y. Sueishi, *Chem. Commun.* 1985, **026**, 903-904.

[11] T. Asano, T. Okada, . *J. Org. Chem* 1986, **51**, 4454-4458.

[12] K.S. Schanze, T.F. Mattox, D.G. Whitten, *J.Org. Chem* 1983, **48**, 2808-2813.

[13] Z.F. Liu, K. Morigaki, T. Enomoto, K. Hashimoto, A. Fujishima, *J. Phys. Chem.* 1992, **96**, 1875-1880.

[14] K.G. Yager, C.J. Barrett, *J. Photochem. Photobiol. A: Chemistry* 2006, **182**, 250-261.

[15] M. Irie, *Chem. Rev.* 2000, **100**, 1683-1684.

[16] M. B. Sponsler in *Optical Sensors and Switches*, (Eds: V. Ramamurthy, K. S. Schanze), Marcel Dekker, New York and Basel, 2001, Chapter 8.

[17] R.H. El Halabieh, O.Mermut, C.J. Barrett *Pure Appl Chem* 2004, **76**,1445-1465.

[18] V. Balzani, A. Credi, M. Venturi, *Molecular devices and machines. A journey into the nanoworld.* Wiley-VCH Weinheim 2003

[19] J. Dokic, M. Gothe, J. Wirth, M. V. Peters, J. Schwartz, S. Hecht, P. Saalfrank, *J. Phys Chem. A* 2009, **113**, 6763-6773.

[20] K.M. Tait, J.A. Parkinson, S.P. Bates, W.J. Ebenezer, A.C. Jones, *J. Photochem. Photobiol. A: Chemistry* 2003, **154**, 179-188.

[21] K.M. Tait, J.A. Parkinson, D.I. Gibson, P.R. Richardson, W.J. Ebenezer, M.G. Hutchings, A.C. Jones, *Photochem. Photobiol. Sci.* 2007, **6**, 1010-1018.

[22] K.M. Tait, J.A. Parkinson, A.C. Jones, W.J. Ebenezer, S.P. Bates, *Chem. Phys. Lett.* 2003, **374**, 372-380.

[23] Gaussian 03, Revision B.02, M. J. Frisch, G. W. Trucks, H. B. Schlegel, G. E. Scuseria, M. A. Robb, J. R. Cheeseman, J. A. Montgomery, Jr., T. Vreven, K. N. Kudin, J. C. Burant, J. M. Millam, S. S. Iyengar, J. Tomasi, V. Barone, B. Mennucci, M. Cossi, G. Scalmani, N. Rega, G. A. Petersson, H. Nakatsuji, M. Hada, M. Ehara, K. Toyota, R. Fukuda, J. Hasegawa, M. Ishida, T. Nakajima, Y. Honda, O. Kitao, H. Nakai, M. Klene, X. Li, J. E. Knox, H. P. Hratchian, J. B. Cross, V. Bakken, C. Adamo, J. Jaramillo, R. Gomperts, R. E. Stratmann, O. Yazyev, A. J. Austin, R. Cammi, C. Pomelli, J. W. Ochterski, P. Y. Ayala, K. Morokuma, G. A. Voth, P. Salvador, J. J. Dannenberg, V. G. Zakrzewski, S. Dapprich, A. D. Daniels, M. C. Strain, O. Farkas, D. K. Malick, A. D. Rabuck, K. Raghavachari, J. B. Foresman, J. V. Ortiz, Q. Cui, A. G. Baboul, S. Clifford, J. Cioslowski, B. B. Stefanov, G. Liu, A. Liashenko, P. Piskorz, I. Komaromi, R. L. Martin, D. J. Fox, T. Keith, M. A. Al-Laham, C. Y. Peng, A. Nanayakkara, M. Challacombe, P. M. W. Gill, B. Johnson, W. Chen, M. W. Wong, C. Gonzalez, and J. A. Pople, Gaussian, Inc., Wallingford CT, 2004.

[24] A.D. Becke, *Phys. Rev. A* 1988, **38**, 3098.

[25] C. Lee, W. Yang, R.G. Parr, *Phys. Rev. B* 1988, **37**, 785.

[26] S. Mierts, E. Scrocco, J. Tomasi, *Chem. Phys.* 1981, **55**, 117-129.

[27] M. Cossi, G. Scalmani, N. Rega, V. Barone, *J. Chem. Phys.* 2002, **117**, 43-54.

[28] 28.M.Poprawa-Smoluch, J. Baggerman, H. Zhang, H.P.A Maas, L. DeCola, A.M. Brouwer, *J. Phys. Chem. A* 2006, **110**, 11926-11937.

[29] K.Matczyszyn, W.Bartkowiak, J. Leszczynki, *J. Mol. Struct.* 2001, **565-566**, 53-57.

[30] C. Reichardt, *Angew. Chem., Int. Ed. Engl.* 1965, **4,** 29-40.

[31] G.P. Ralph, *J. Chem. Phys* 1952, **20**, 1478-1480.